

<https://doi.org/10.1038/s41522-025-00745-3>

# *Lactobacillus* regulate muscle fiber type conversion in Chinese native pigs via tryptophan metabolism



Bo Song<sup>1,2</sup>, Md. Abul Kalam Azad<sup>1,2</sup>, Qian Zhu<sup>1,2</sup>, Yating Cheng<sup>1,2</sup>, Sujuan Ding<sup>1,3</sup>, Kang Yao<sup>1,2</sup> & Xiangfeng Kong<sup>1,2</sup>✉

Identifying potential gut microbes and metabolites that can influence muscle fiber type is gaining interest in meat quality research. In this study, muscle fiber characteristics, muscle metabolite profiles, and gut microbiota and metabolome were compared among three pig breeds (Taoyuan black, TB; Xiangcun black, XB; and Duroc pigs). The results showed that the slow-twitch fiber percentage was higher ( $P < 0.05$ ) in native pigs (TB and XB pigs) compared to Duroc pigs. The differences were mainly regulated by *Lactobacillus* abundance and tryptophan metabolism. Further, fecal microbiota transplantation from XB pigs transferred a higher slow-twitch fiber percentage, *Lactobacillus* abundance, kynurenic acid level, and *AMPK/PGC-1 $\alpha$*  expression to mice. These findings suggest that *Lactobacillus* in the colon of TB and XB pigs, through kynurenic acid production, may promote slow-twitch fiber formation via the *AMPK/PGC-1 $\alpha$*  signaling pathway.

Skeletal muscle is characterized by high heterogeneity and plasticity, attributed to its composition of different types of muscle fibers. The muscle fibers can be classified into four types based on the isoforms of myosin heavy-chain (MyHC), including type I (slow-oxidative), type IIa (fast-oxidative), type IIx (intermediate), and type IIb (fast-glycolytic)<sup>1</sup>. These muscle fibers can be transformed under specific physiological conditions in the order of type I→type IIa→type IIx→type IIb, or vice versa<sup>2</sup>. In livestock meat quality research, it is widely accepted that animals with a higher proportion of oxidative muscle fibers (type I and IIa) have better meat quality<sup>3</sup>. Previous studies have found that native pig breeds have a higher proportion or expression of oxidative muscle fibers compared to commercial pigs. For instance, compared with Landrace pigs, the mRNA expressions of *MyHC I* and *MyHC IIa* were higher in Jinhua pigs<sup>4</sup>; the expression of *MyHC I* was also higher in Bama Xiang pigs<sup>5</sup>. Furthermore, the Korean native black pigs have shown a higher expression of *MyHC I* than the Landrace pigs<sup>6</sup>. Therefore, exploring the mechanism of slow-twitch fiber formation through the characteristics of native pigs could provide valuable insights for strategies aimed at improving meat quality.

The gastrointestinal tract of large animals harbors a vast and complex microbial community that plays a crucial role in the digestion and absorption of nutrients, and regulates gut health<sup>7</sup>. Additionally, the gut microbiota influences peripheral tissue metabolism and metabolic diseases

through the production of different bioactive compounds, such as branched-chain amino acids, short-chain fatty acids, and bile acids<sup>8</sup>. The gut microbiota and gut microbiota-derived metabolites also significantly influence muscle physiology and function. Studies have shown that germ-free mice exhibit muscle atrophy and downregulation of genes associated with muscle growth and mitochondrial function, compared to specific pathogen-free mice<sup>9</sup>. Probiotic *Lactobacillus casei* Shirota administration to mice has been shown to mitigate age-induced muscle mass loss, strength reduction, and mitochondrial dysfunction<sup>10</sup>. In pigs, germ-free pigs have been found to exhibit reduced muscle mass, while fecal microbiota transplantation (FMT) from normal pigs can partially restore muscle growth and development<sup>11</sup>. These findings suggest that gut microbes and their metabolites are important for the maintenance of skeletal muscle growth and function.

Native pigs exhibit significant differences from commercial pigs not only in muscle fiber composition but also in their gut microbiota. For instance, Jinwu pigs have a higher abundance of fiber-digesting genera in the colon, such as *Treponema* and *Terrisporobacter*, compared to Duroc × Landrace × Yorkshire (DLY) pigs under roughage feeding<sup>12</sup>. Similarly, Shaziling pigs showed a higher abundance of beneficial bacteria, such as *Lactobacillus johnsonii* and *Lactobacillus amylovorus*, in the ileum than Yorkshire pigs<sup>13</sup>. Moreover, the abundances of Firmicutes, Bacteroidetes,

<sup>1</sup>National Engineering Laboratory for Pollution Control and Waste Utilization in Livestock and Poultry Production, Hunan Provincial Key Laboratory of Animal Nutritional Physiology and Metabolic Process, Institute of Subtropical Agriculture, Chinese Academy of Sciences, Changsha, China. <sup>2</sup>College of Advanced Agricultural Sciences, University of Chinese Academy of Sciences, Beijing, China. <sup>3</sup>College of Bioscience and Biotechnology, Hunan Agricultural University, Hunan Engineering Laboratory for Pollution Control and Waste Utilization in Swine Production, Changsha, Hunan, 410128, China. ✉e-mail: [nrxkf@isa.ac.cn](mailto:nrxkf@isa.ac.cn)

Tenericutes, Spirochaetes, Fusobacteria, and Kiritimatiellaeota in the ileum of Ningxiang pigs are lower than those in DLY pigs<sup>14</sup>. Xiangcun black (XB) pig is a crossbreed derived from Taoyuan black pigs (TB, the maternal line) and Duroc pigs (the paternal line). Our previous study indicated that TB and XB pigs have higher slow-twitch fiber percentages and better meat quality than the Duroc pigs during the finishing stage<sup>15</sup>. Additionally, the microbiota composition in the ileum of TB and XB pigs differs from that in Duroc pigs during suckling and weaning periods<sup>16</sup>. However, the mechanistic links between gut microbiota and muscle fiber type development, which are critical for meat quality traits, remain unexplored. Therefore, studying these three breeds (TB, XB, and Duroc pigs) during the growing stage allows us to uncover the potential mechanisms by which gut microbiota in Chinese native pig breeds shape superior meat quality during development.

Given the presence of the gut-muscle axis, we hypothesized that the gut microbiota of TB and XB pigs may regulate the formation of slow-twitch fibers. Thus, the present study selected growing TB, XB, and Duroc pigs to identify core gut microbes and metabolites that might regulate the formation of muscle slow-twitch fibers and further validate their effects through FMT. The findings will provide references for the regulation of livestock meat quality.

## Results

### TB and XB pigs have higher slow-twitch fiber percentages, and muscular differential metabolites are enriched in the malate-aspartate shuttle pathway

The muscle fiber characteristics and targeted metabolome of three pig breeds are shown in Fig. 1. Representative images of the three pig breeds are shown in Fig. 1A. At 80 days of age, XB pigs exhibited a higher ( $P < 0.05$ ) slow-twitch fiber percentage compared to TB and Duroc pigs; at 125 days of age, the slow-twitch fiber percentage remained higher ( $P < 0.05$ ) in XB and TB pigs compared to Duroc pigs (Fig. 1B, C). The cross-sectional area of muscle fibers was smaller ( $P < 0.05$ ) in TB pigs than in Duroc pigs at 80 days of age (Fig. 1C). Additionally, the cross-sectional area of muscle fibers was smaller ( $P < 0.05$ ) in XB and TB pigs than in Duroc pigs at 125 days of age (Fig. 1C). Furthermore, the *MyHC Ila* expression was upregulated ( $P < 0.05$ ) in TB and XB pigs relative to Duroc pigs at 80 days of age. At 125 days of age, the *MyHC I* expression was upregulated ( $P < 0.05$ ), and *MyHC Iib* expression was downregulated ( $P < 0.05$ ) in TB and XB pigs compared to Duroc pigs (Fig. 1D). Moreover, *MyHC Ila* expression was significantly higher ( $P < 0.05$ ) in TB pigs than in Duroc pigs at 125 days of age.

The targeted metabolomics approach detected 207 metabolites in muscle tissues of the three pig breeds. The PLS-DA shows that at both 80 and 125 days of age, the muscle metabolite profiles of TB and XB pigs formed distinct clusters from those of Duroc pigs (Fig. 1E, F). At 80 and 125 days of age, there were 88 and 51 significant differentially abundant muscle metabolites, respectively, among the pig breeds. The top 50 differentially abundant metabolites at each age are illustrated in Fig. 1G, H. Further pathway analysis indicated that these differential metabolites were significantly enriched in several pathways, including aspartate metabolism, malate-aspartate shuttle, urea cycle, and phenylalanine and tyrosine metabolism at both 80 and 125 days of age (Fig. 1I, J).

### TB and XB pigs have higher *Lactobacillus* abundance, which is positively correlated with slow-twitch fiber percentage

To explore the differences in gut microbial composition among the three pig breeds and their association with muscle fiber composition, 16S rRNA sequencing was conducted on colonic contents. Although alpha-diversity did not differ among the breeds at 80 days of age, the Shannon, Simpson, and Observed species indices of Duroc pigs were higher ( $P < 0.05$ ) at 125 days of age than those of XB pigs (Supplementary Figure 1). The PCoA score plots indicate that the gut microbiota composition of TB and XB pigs tended to be clustered separately from those of Duroc pigs (Fig. 2A, K). However, the PCoA analysis revealed an outlier in the 125-day-old Duroc pigs, and this outlier was excluded from subsequent microbial data analyses.

LEfSe analysis identified characteristic genera for each pig breed at different ages. At 80 days of age, Duroc pigs were distinguished by the presence of *Ralstonia*, *Campylobacter*, and *Mycobacterium* (Fig. 2B). The characteristic genera for TB pigs were *Corynebacterium*, *Staphylococcaceae\_Staphylococcus*, *Dietzia*, and *Leifsonia* (Fig. 2B). XB pigs were characterized by high levels of *Lactobacillus* and *Bifidobacterium* (Fig. 2B). At 125 days of age, the characteristic genera for Duroc pigs included *Gemella*, *Rothia*, *Rhodococcus*, *Turicibacter*, *Corynebacterium*, *Psychrobacter*, *Wolbachia*, *Burkholderia*, *Peptostreptococcus*, *Facklamia*, *Actinomyces*, *Acidovorax*, *Parvimonas*, and *Dermatophilus* (Fig. 2L). The characteristic genera for XB pigs were *Lactobacillus* (Fig. 2L). However, no characteristic genera were identified for TB pigs at 125 days of age.

At the genus level, 7 (Fig. 2C–I) and 12 (Fig. 2M–X) of the top 20 most abundant genera showed significant differences among the breeds at 80 and 125 days, respectively. At 80 days of age, *Lactobacillus* and *Dietzia* abundances were higher ( $P < 0.05$ ) in TB and XB pigs than in Duroc pigs. Conversely, *Ralstonia* and *Campylobacter* abundances were higher ( $P < 0.05$ ) in Duroc pigs than in the other two breeds. In addition, *Staphylococcaceae\_Staphylococcus* abundance was higher ( $P < 0.05$ ) in TB pigs compared with Duroc and XB pigs, as well as *Bifidobacterium* abundance in XB pigs compared with Duroc and TB pigs. Moreover, *Corynebacterium* abundance was higher ( $P < 0.05$ ) in TB pigs than in Duroc pigs (Fig. 2C–I). At 125 days of age, *Lactobacillus* and *Allobaculum* abundances were higher ( $P < 0.05$ ) in TB and XB pigs than in Duroc pigs. Duroc pigs had higher ( $P < 0.05$ ) *Peptostreptococcus* and *Facklamia* abundances than the other two breeds. Additionally, Duroc pigs had higher ( $P < 0.05$ ) abundances than XB pigs for the following genera: *Gemella*, *SMB53*, *Turicibacter*, *Rothia*, *Rhodococcus*, *Corynebacterium*, *Burkholderia*, and *Actinomyces* (Fig. 2M–X).

Correlation analysis revealed that the *Dietzia* abundance in the colon was positively ( $P < 0.05$ ) correlated with *Corynebacterium*. The slow-twitch fiber percentage was positively ( $P < 0.05$ ) correlated with *Lactobacillus* and *Bifidobacterium* abundances at 80 days of age (Fig. 2J). Additionally, the *MyHC Iix* expression was positively ( $P < 0.05$ ) correlated with *Dietzia*, as well as *MyHC Iib* with *Dietzia* and *Corynebacterium*. At 125 days of age, the correlations between colonic differential genera were categorized into two groups (Fig. 2Y), of which *Lactobacillus* was negatively ( $P < 0.05$ ) correlated with the remaining differential genera, and most of these remaining genera were positively ( $P < 0.05$ ) correlated with each other. Regarding the correlations between muscle fiber characteristics and colonic differential genera, the slow-twitch fiber percentage was positively ( $P < 0.05$ ) correlated with *Lactobacillus* abundance, while negatively ( $P < 0.05$ ) correlated with *Gemella*, *SMB53*, *Rothia*, *Rhodococcus*, *Burkholderia*, *Peptostreptococcus*, *Actinomyces*, and *Facklamia* abundances. The muscle fiber cross-sectional area was positively ( $P < 0.05$ ) correlated with *Burkholderia*, *Peptostreptococcus*, and *Actinomyces* abundances, while negatively ( $P < 0.05$ ) correlated with *Allobaculum* abundance. The *MyHC I* expression was positively ( $P < 0.05$ ) correlated with *Lactobacillus* abundance, while negatively ( $P < 0.05$ ) with *Rothia*, *Corynebacterium*, *Peptostreptococcus*, and *Actinomyces* abundances. The *MyHC Ila* expression was positively ( $P < 0.05$ ) correlated with *Allobaculum* abundance, while *MyHC Iix* expression was positively ( $P < 0.05$ ) correlated with *Rhodococcus*, *Burkholderia*, and *Peptostreptococcus* abundances. Moreover, the *MyHC Iib* expression was positively ( $P < 0.05$ ) correlated with *Burkholderia* and *Peptostreptococcus* abundances, while negatively ( $P < 0.05$ ) with *Lactobacillus* abundance.

### Colonic differential metabolites among three pig breeds were significantly enriched in the tryptophan metabolism pathway

The results of colonic metabolite profiles are shown in Fig. 3. A total of 857 metabolites were detected among the breeds. The PLS-DA analysis indicated that the metabolite composition in TB and XB pigs was clustered separately from those of Duroc pigs (Fig. 3A, D). At 80 days of age, there were 232 significantly differential metabolites among three pig breeds. The pathway analysis revealed that these differential metabolites were enriched ( $P < 0.05$ ) in tryptophan metabolism, valine/leucine/isoleucine biosynthesis,

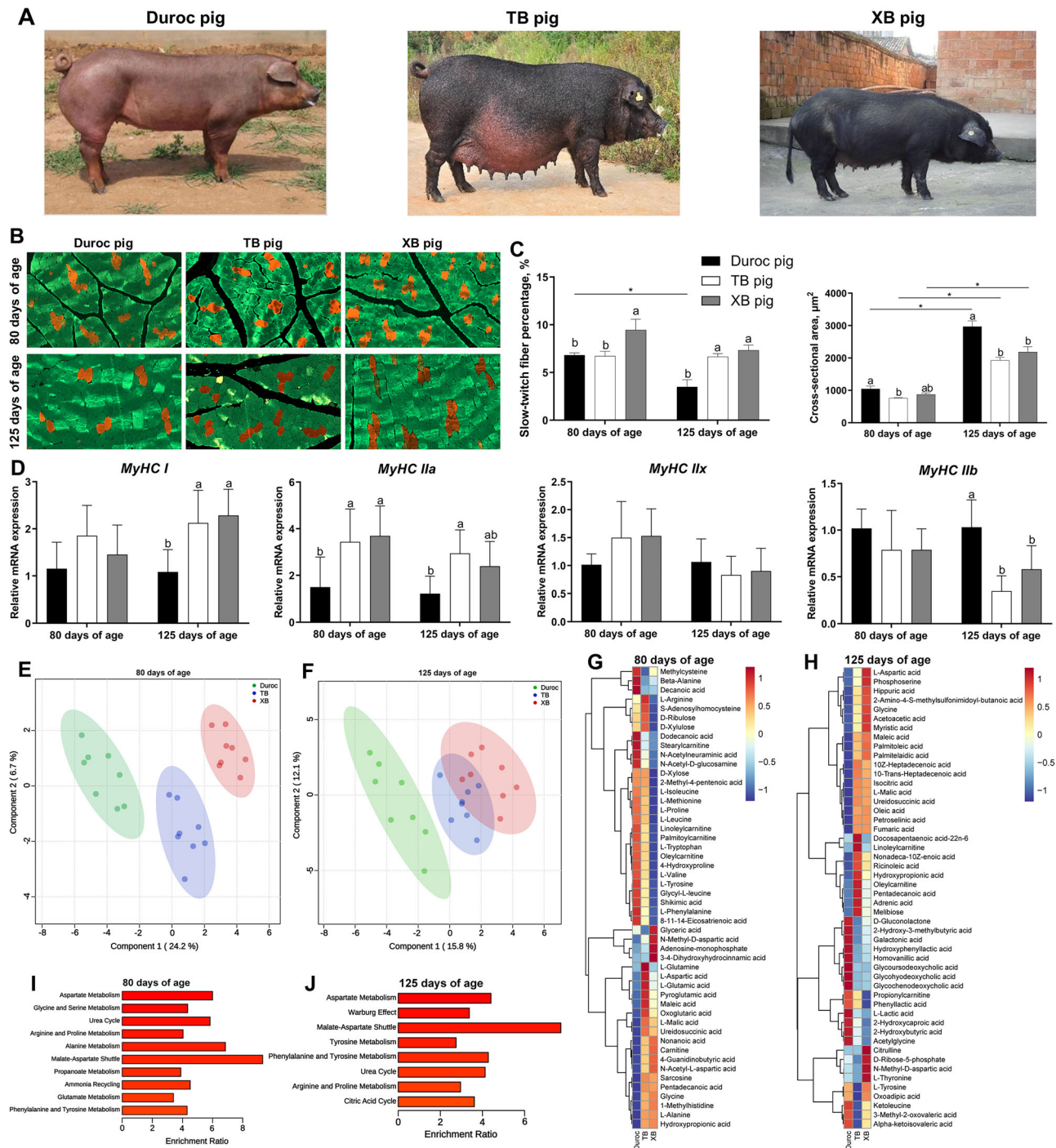


**Fig. 1 | Muscle fiber type and targeted metabolome of three pig breeds at 80 and 125 days of age ( $n = 8$ ).** Data are presented as means with SD. **A** Representative images of three pig breeds, **B** immunofluorescent staining for muscle fiber types, **C** slow-twitch fiber percentage and cross-sectional area, **D** mRNA expression of four myosin-heavy chain (*MyHC*) isoforms, **E**, **F** partial least squares discriminant analysis (PLS-DA) score plots of targeted metabolome in muscle of three pig breeds at 80 and 125 days of age. **G**, **H** Heatmaps of top 50 differential metabolites

concentrations in muscle of three pig breeds at 80 and 125 days of age. **I**, **J** Pathway enrichment analysis of top 50 differential metabolites in *longissimus dorsi* muscle of three pig breeds at 80 and 125 days of age. Different lowercase letters on bars indicate significant differences among pig breeds ( $P < 0.05$ , Tukey's *post-hoc* test). Asterisks denote significant differences between different ages ( $P < 0.05$ , Student's *t* test). TB, Taoyuan black; XB, Xiangcun black.

vitamin B<sub>6</sub> metabolism, pentose and glucuronate interconversions, purine metabolism, pentose phosphate pathway, histidine metabolism, and amino sugar and nucleotide sugar metabolism (Fig. 3B). For the tryptophan metabolism pathway, the identified differential metabolites included oxoadipic acid, N-methyltryptamine, serotonin, 4-(2-aminophenyl)-2,4-dioxobutanoic acid, 3-hydroxyanthranilic acid, N-acetylserotonin, and melatonin (Fig. 3C). Specifically, the concentrations of

3-hydroxyanthranilic acid, N-acetylserotonin, and melatonin were lower ( $P < 0.05$ ), while N-methyltryptamine was higher ( $P < 0.05$ ) in TB and XB pigs than in Duroc pigs. The concentration of serotonin was higher ( $P < 0.05$ ) in XB pigs than in TB and Duroc pigs. Additionally, the concentration of 4-(2-aminophenyl)-2,4-dioxobutanoic acid was higher ( $P < 0.05$ ) in XB pigs than in TB pigs, and oxoadipic acid was higher ( $P < 0.05$ ) in TB pigs than in Duroc pigs.



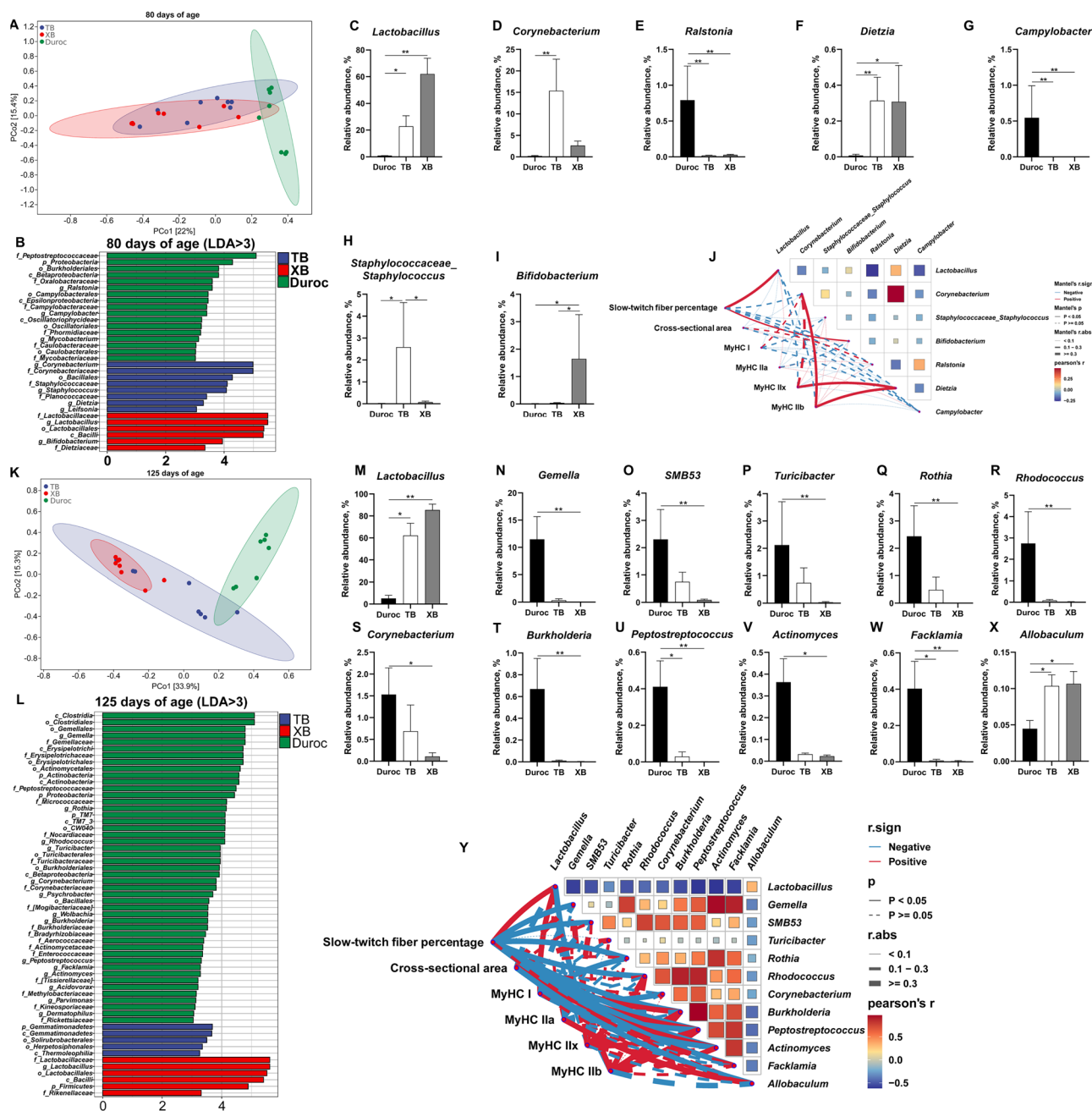


**Fig. 2 | Colonic microbiota of three pig breeds at 80 and 125 days of age** ( $n = 7-8$ ). Data are presented as means with SD. **A** Principal coordinates analysis (PCoA) score plots of gut microbiota of three pig breeds at 80 days of age, **B** linear discriminant analysis effect size (LEfSe) of colonic microbiota of three pig breeds at 80 days of age, **C–I** taxonomic differences of colonic microbiota of three pig breeds at 80 days of age, **J** correlation analysis between differential genera and muscle fiber characteristics of three pig breeds at 80 days of age, **K** PCoA score plots of the colonic

gut microbiota of three pig breeds at 125 days of age, **L** LEfSe of colonic microbiota of three pig breeds at 125 days of age, **M–X** taxonomic differences of colonic microbiota of three pig breeds at 125 days of age, and **Y** correlation analysis between differential genera and muscle fiber characteristics of three pig breeds at 125 days of age. \* $P < 0.05$ ; \*\* $P < 0.01$  (Kruskal–Wallis test). TB, Taoyuan black; XB, Xiangcun black.

At 125 days of age, there were 286 differential metabolites among the three breeds. The pathway analysis revealed that differential metabolites were predominantly enriched in arginine biosynthesis, nicotinate and nicotinamide metabolism, histidine metabolism, tryptophan metabolism, and amino sugar and nucleotide sugar metabolism (Fig. 3E). For the tryptophan metabolism pathway, the identified differential metabolites included tryptamine, L-kynurenine, N-acetylserotonin, melatonin, 6-hydroxymelatonin, 5-hydroxyindoleacetic acid, and kynurenic acid (Fig. 3F). Moreover, the concentrations of tryptamine and L-kynurenine were higher ( $P < 0.05$ ) in TB pigs than in XB and Duroc pigs. The concentrations of N-acetylserotonin and 6-hydroxymelatonin were higher

( $P < 0.05$ ) in TB and Duroc pigs than in XB pigs. The XB pigs had a lower ( $P < 0.05$ ) concentration of 5-hydroxyindoleacetic acid than the Duroc pigs. The concentration of melatonin was higher ( $P < 0.05$ ) in XB pigs than in Duroc pigs, yet lower ( $P < 0.05$ ) than in TB pigs.

### TB and XB pigs have higher kynurenic acid level and upregulated AMPK/PGC-1 $\alpha$ pathway

To determine whether the colonic microbiota and metabolite variations among the three pig breeds influence the host's kynurenine and kynurenic acid metabolism, we analyzed the concentrations of these compounds in the serum, colonic contents, liver, and muscle of pigs at 125 days of age. As shown

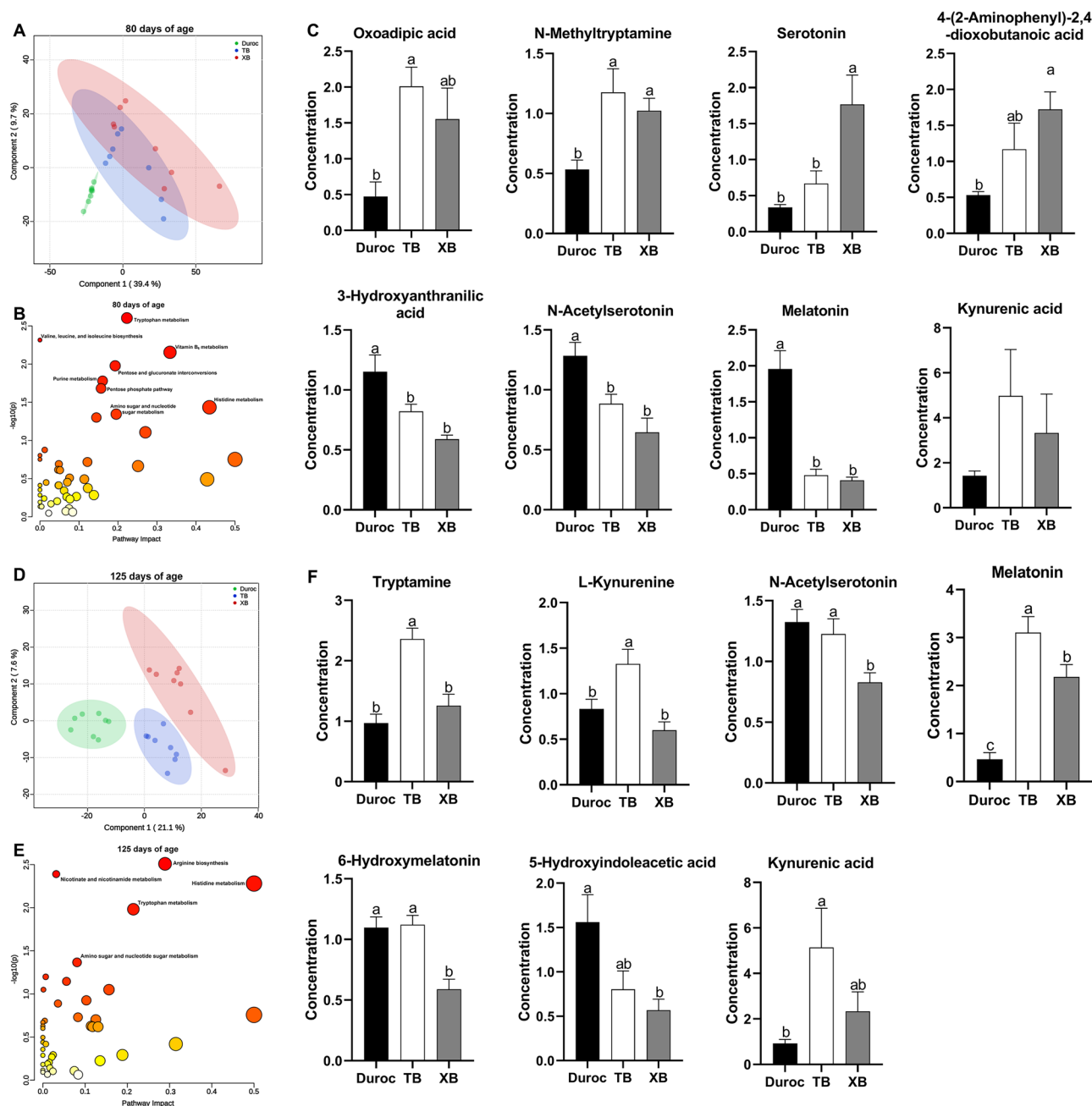


**Fig. 3 | Colonic metabolome of three pig breeds at 80 and 125 days of age ( $n = 8$ ).** Data are presented as means with SD. **A, D** Partial least squares discriminant analysis (PLS-DA) score plots of colonic metabolome of three pig breeds at 80 and 125 days of age. **B, E** pathway analysis of differential metabolites in the colon of three pig breeds

at 80 and 125 days of age. **C, F** concentrations of tryptophan metabolism-related differential metabolites in colon of three pig breeds at 80 and 125 days of age. Different lowercase letters on bars indicate significant differences among pig breeds ( $P < 0.05$ , Tukey's *post hoc* test). TB, Taoyuan black; XB, Xiangcun black.

in Fig. 4, no significant differences were observed in kynurenine concentration in the serum, colonic contents, liver, and muscle among the three pig breeds (Fig. 4A–D). However, consistent with the metabolomics data, the colonic concentration of kynurenic acid was higher ( $P < 0.05$ , Fig. 4B) in TB and XB pigs compared to Duroc pigs. Additionally, the TB and XB pigs displayed increasing trends in serum ( $P = 0.058$ ) and muscle ( $P = 0.078$ ) kynurenic acid concentration compared with Duroc pigs (Fig. 4C, D).

The mRNA expression of genes related to kynurenine metabolism and muscle fiber type transformation in muscle were analyzed. The results showed no significant differences in indoleamine 2,3-dioxygenase 1 (*IDO1*), kynurenine aminotransferase 1 (*KYAT1*), *KYAT2*, *KYAT3*, and *KYAT4* expressions among the three breeds (Fig. 4E–I). Conversely, the protein kinase AMP-activated catalytic subunit alpha 1 (*AMPK*) expression displayed

an increasing trend ( $P = 0.052$ ; Fig. 4J), while peroxisome proliferator-activated receptor gamma coactivator 1 alpha (*PGC-1α*) expression was upregulated ( $P < 0.05$ ) in TB and XB pigs compared to Duroc pigs (Fig. 4K).

#### **Lactobacillus is the core genus associated with tryptophan metabolism**

The above results indicated more significant differences in colonic microbiota and metabolite composition between XB and Duroc pigs. To identify core bacterial genera associated with tryptophan metabolism, we analyzed the correlations between the top 50 most abundant bacterial genera and all tryptophan metabolites in the colon of XB and Duroc pigs. The results showed that, at both 80 and 125 days of age, *Lactobacillus* had the highest number of significant correlations with tryptophan metabolites ( $P < 0.05$

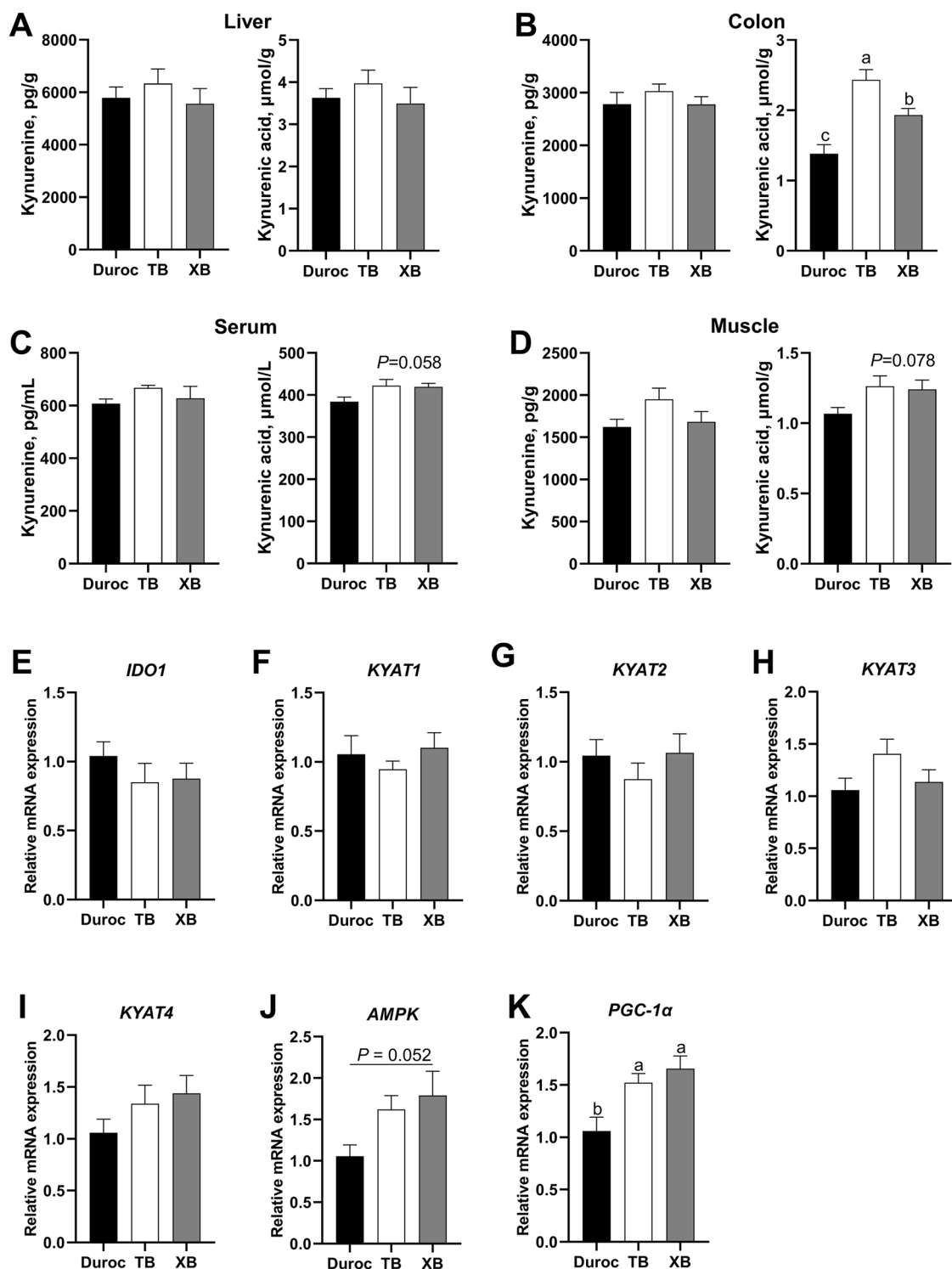


**Fig. 4 | Kynurenine and kynurenic acid concentrations and gene expression analysis of three pig breeds at 125 days of age ( $n = 8$ ).** Data are presented as means with SD. Kynurenine and kynurenic acid concentrations in **A** liver, **B** colon, **C** serum, and **D** muscle. The mRNA expressions of **E** indoleamine 2,3-dioxygenase 1 (*IDO1*), **F** kynurenine aminotransferase 1 (*KYAT1*), **G** *KYAT2*, **H** *KYAT3*, **I** *KYAT4*,

**J** protein kinase AMP-activated catalytic subunit alpha 1 (*AMPK*), and **K** peroxisome proliferator-activated receptor gamma coactivator 1 alpha (*PGC-1α*) in the muscle. Different lowercase letters on bars indicate significant differences among pig breeds ( $P < 0.05$ , Tukey's *post hoc* test). TB, Taoyuan black; XB, Xiangcun black.

and  $|r| \geq 0.5$ ). In the correlation network analysis, *Lactobacillus* consistently occupied a central position (Fig. 5A, B). Therefore, *Lactobacillus* is a core bacterial genus in pig gut microbiota associated with tryptophan metabolism. Moreover, *Lactobacillus* was positively correlated with kynurenic acid at both 80 and 125 days of age, while negatively correlated with kynurenine at 80 days of age.

#### FMT from XB pigs tended to increase the slow-twitch fiber percentage in mice

Fecal microbiota from XB and Duroc pigs at 125 days of age were transplanted into mice to assess the impact of FMT from different pig breeds on muscle fiber composition in mice. The results indicated that FMT had no significant influence ( $P > 0.05$ ) on the body weight (Fig. 6A) and serum

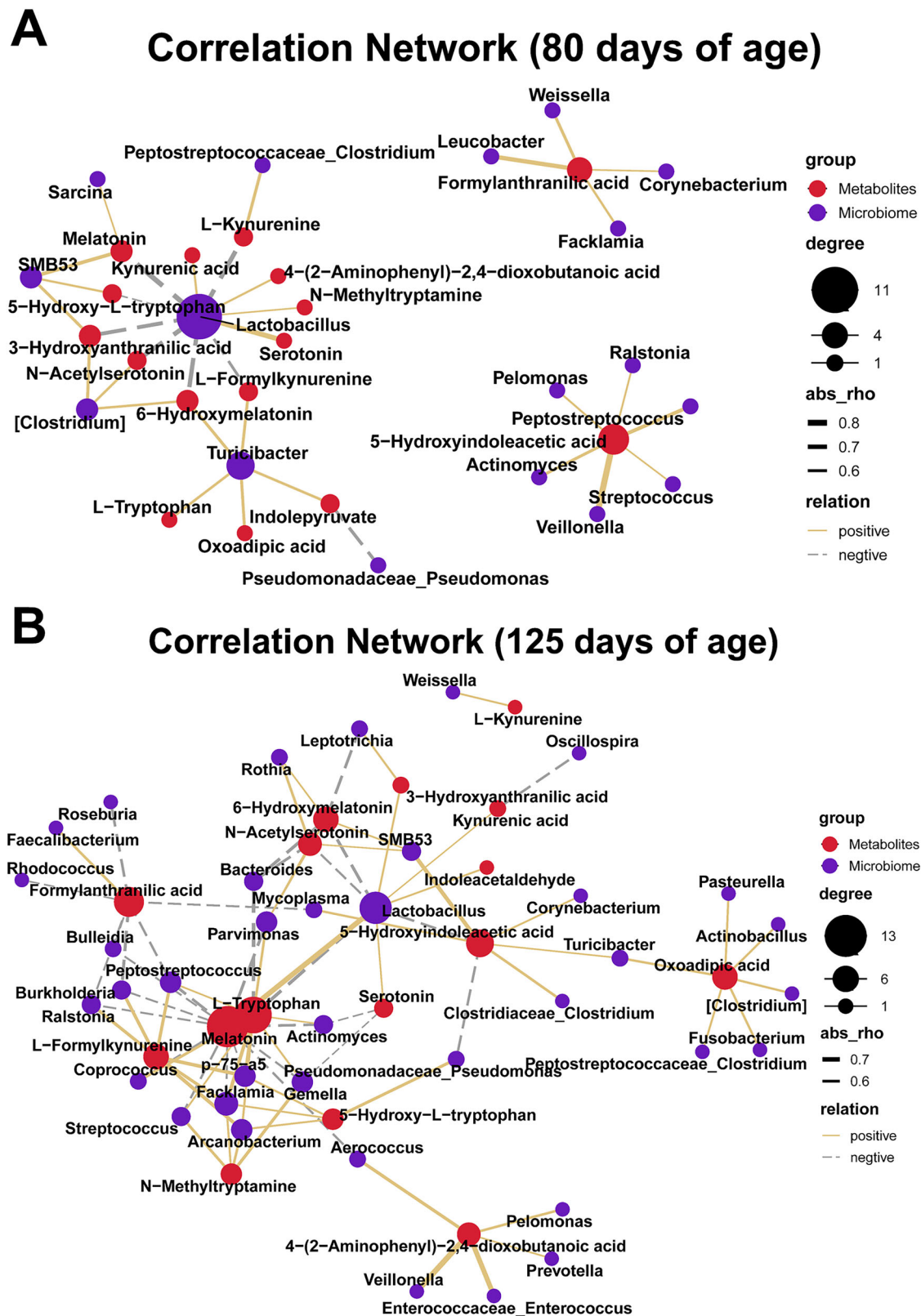


**Fig. 5 | Correlation network between top 50 most abundant genera and tryptophan metabolites ( $n = 8$ ). Note:** Correlation network between top 50 most abundant genera and tryptophan metabolites in XB and Duroc pigs at **A** 80 and **B** 125 days of age. The color of the dots represents metabolites or genera, the dot size

indicates the number of significantly correlated metabolites or genera ( $P < 0.05$  and  $|r| \geq 0.5$ ), the line thickness reflects the correlation strength, solid lines denote positive correlations, and dashed lines represent negative correlations.

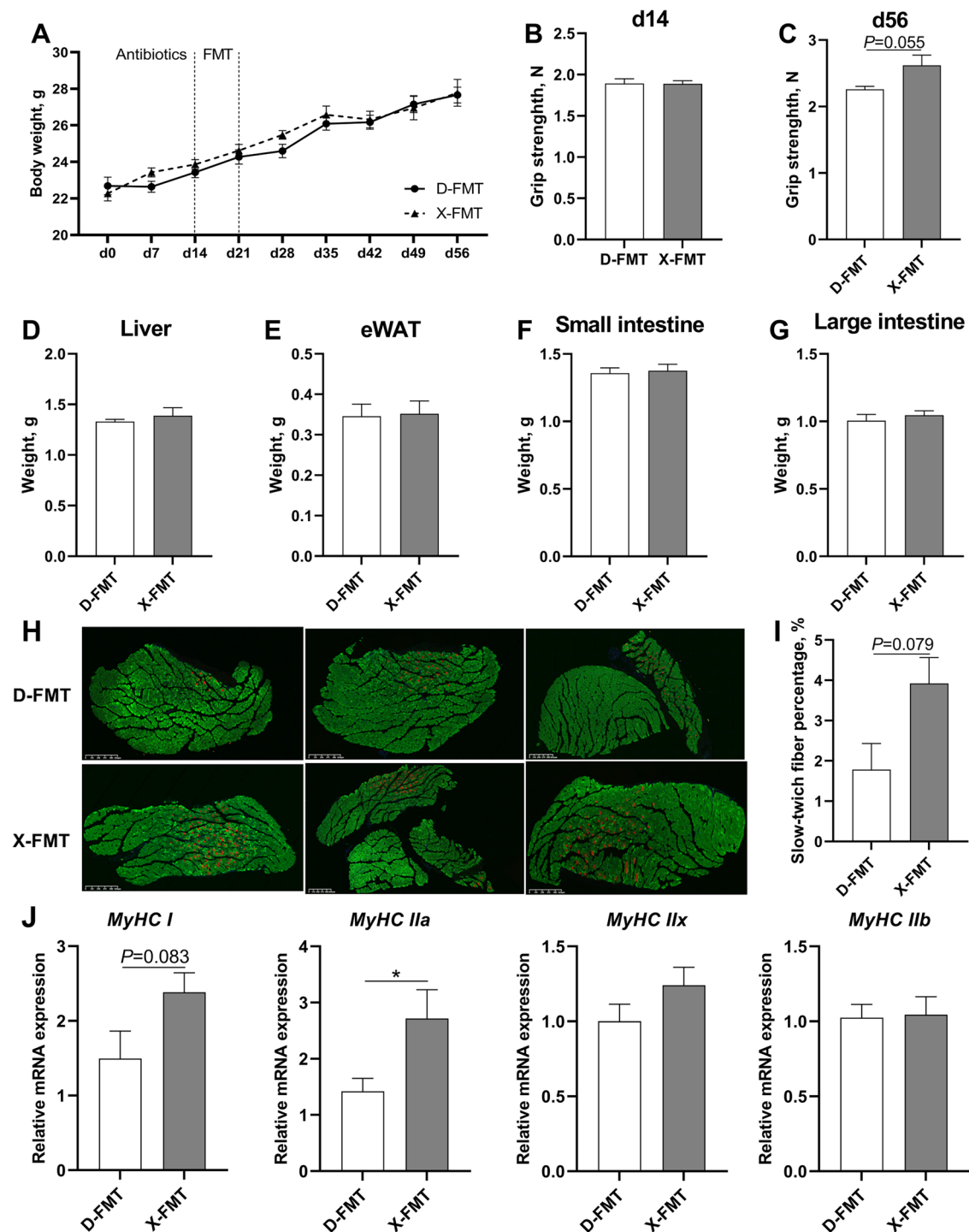


**Fig. 6 | The effects FMT from XB and Duroc pigs on the growth performance, grip strength, organ weight, and muscle fiber type of mice ( $n = 5$ ). Data are presented as means with SD. **A** Growth performance and **B**, **C** grip strength, **D** liver weight, **E** epididymal white adipose tissue (eWAT) weight, **F** small intestine weight, and **G** large intestine weight. **H** immunofluorescent staining for muscle fiber types;**

**I** slow-twitch fiber percentage. **J** The mRNA expression of four myosin heavy-chain (*MyHC*) isoforms. \* $P < 0.05$  (Students' *t* test). D-FMT mice received fecal microbiota transplantation from Duroc pigs at 125 days of age, and X-FMT mice received fecal microbiota transplantation from Xiangcun black (XB) pigs at 125 days of age.

biochemical parameters (Table 1) of the mice. At day 14 (after a 2-week antibiotic regimen), grip strength remained unchanged (Fig. 6B). However, at day 56 (five weeks post-FMT), the X-FMT mice displayed an increasing trend in grip strength ( $P = 0.055$ ) compared with D-FMT mice (Fig. 6C). No significant differences ( $P > 0.05$ ) were observed in organ weights, including the liver, eWAT, small intestine, and large intestine, between X-FMT and

D-FMT mice (Fig. 6D–G). Slow-twitch fiber percentage ( $P = 0.079$ ) and *MyHC I* expression ( $P = 0.083$ ) in muscle of X-FMT mice displayed an increasing trend compared with D-FMT mice (Fig. 6H and 6J). Additionally, expression of *MyHC IIa* was significantly upregulated ( $P < 0.05$ ) in X-FMT mice, whereas no significant differences ( $P > 0.05$ ) were observed in *MyHC IIx* and *MyHC IIb* expressions (Fig. 6J).



**Table 1 | Serum biochemical parameters of D-FMT and X-FMT mice**

Items	D-FMT	X-FMT	SEM	P-values
ALB, g/L	22.30	22.68	0.54	0.75
ALT, U/L	20.62	22.72	1.30	0.45
AST, U/L	111.40	105.40	9.79	0.78
CHE, U/L	2792.60	3061.60	84.04	0.11
CHO, mmol/L	1.96	2.10	0.07	0.33
CK, U/L	1242.20	1525.40	197.46	0.51
CREA, $\mu$ mol/L	5.00	6.60	0.79	0.34
HDL-C, mmol/L	1.50	1.53	0.04	0.68
LA, mmol/L	10.11	9.71	0.54	0.73
LDH, U/L	492.20	652.80	73.93	0.30
LDL-C, mmol/L	0.20	0.20	0.01	0.80
LIP, U/L	65.40	34.24	17.53	0.41
AMM, $\mu$ mol/L	241.18	217.10	14.63	0.44
TG, mmol/L	0.96	1.25	0.10	0.16
TP, g/L	33.72	36.08	0.78	0.14
UN, mmol/L	4.06	4.46	0.19	0.32

Data are expressed as means with SEM ( $n = 5$ ).

ALB albumin, ALT alanine aminotransferase, AST aspartate aminotransferase, CHE cholinesterase, CHO cholesterol, CK creatine kinase, CREA creatinine, HDL-C high-density lipoprotein-cholesterol, LA lactic acid, LDH lactate dehydrogenase, LDL-C low-density lipoprotein-cholesterol, LIP lipase, AMM ammonia, TG triglycerides, TP total protein, UN urea nitrogen.

### FMT from XB pigs increased the *Lactobacillus* abundance in the colon of mice

To confirm the effectiveness of FMT on mice, we analyzed the colonic microbiota composition in X-FMT and D-FMT mice. The PCoA score plots revealed that the microbiota composition of X-FMT and D-FMT mice clustered separately (Fig. 7A). The LEfSe analysis identified *Bifidobacterium*, *Parabacteroides*, *Bacteroides*, *Lactococcus*, and *Mucispirillum* as characteristic genera in the D-FMT mice (Fig. 7B). In line with the microbiota profile of XB pigs at 125 days of age, *Lactobacillus* was the predominant signature genus in the X-FMT mice, accompanied by *Lachnospiraceae\_Clostridium* and *Coprobaecillus* (Fig. 7B). The taxonomic differences of the top 20 genera demonstrated that the abundances of *Lactobacillus* and *Lachnospiraceae\_Clostridium* were higher ( $P < 0.01$ , Fig. 7C) in X-FMT mice compared to D-FMT mice. Conversely, the abundances of *Bacteroides*, *Bifidobacterium*, *Parabacteroides*, and *Mucispirillum* were lower ( $P < 0.01$ , Fig. 7C) in X-FMT mice than in D-FMT mice.

### FMT from XB pigs increased Kynurenic acid level and upregulated the AMPK/PGC-1 $\alpha$ pathway in mice

The results of hepatic kynurenine and kynurenic acid concentrations showed no significant differences between X-FMT and D-FMT mice (Fig. 8A). However, colonic kynurenic acid concentration was higher ( $P < 0.05$ , Fig. 8B), while serum kynurenine concentration ( $P = 0.083$ ) displayed a decreasing trend (Fig. 8C) in X-FMT mice compared with D-FMT mice. Additionally, muscle kynurenic acid concentration ( $P = 0.066$ ) displayed an increasing trend in X-FMT mice than in D-FMT mice (Fig. 8D). Gene expression analysis of the *gastrocnemius* muscle revealed no significant differences ( $P > 0.05$ ) in the mRNA levels of *IDO1*, *KYAT1*, *KYAT2*, *KYAT3*, and *KYAT4* between X-FMT and D-FMT mice (Fig. 8E, I). Notably, AMPK expression was significantly upregulated ( $P < 0.05$ ) in X-FMT mice compared to D-FMT mice (Fig. 8J), while PGC-1 $\alpha$  expression tended to be upregulated ( $P = 0.079$ ) (Fig. 8K).

## Discussion

Muscle tissue, crucial for locomotion and protection, significantly influences the quality of meat from livestock<sup>17</sup>. The present study focused on the gut microbiota and gut microbiota-derived metabolites in pigs with distinct muscle fiber compositions. Through multi-omics analyses, we demonstrated that the colonic biomarker *Lactobacillus* and kynurenic acid could potentially promote the formation of slow-twitch fibers in TB and XB pigs. Consequently, FMT from XB and Duroc pigs into mice validated the role of colonic *Lactobacillus* and kynurenic acid in the formation of slow-twitch fibers and associated metabolic regulatory pathways.

Globally, native pig breeds, which have not undergone selective breeding, tend to have a higher slow-twitch fiber percentage than commercial breeds that have been selected for traits like growth rate and leanness. The present study revealed that, during the growing period, TB and XB pigs have significantly higher slow-twitch fiber percentages and *MyHC I* and *MyHC IIa* expressions than Duroc pigs. Consistent with our findings, the Rongchang pig, a Chinese native breed, exhibited higher *MyHC I* and *MyHC IIa* expressions in the muscles than Landrace pig<sup>18</sup>. Similarly, the Mongcai pig from Vietnam has higher expressions of these genes than Pietrain and Duroc pigs<sup>19</sup>. Moreover, Korean native pigs also demonstrated higher *MyHC I* and *MyHC IIa* expressions than Landrace and Yorkshire pigs<sup>20</sup>. Our previous findings indicated that the meat quality of finishing TB and XB pigs was superior to Duroc pigs in terms of pH, color, tenderness, and intramuscular fat content, and they had a correspondingly higher slow-twitch fiber percentage<sup>15</sup>. Taken together, it is evident that native pig breeds generally have a higher slow-twitch fibers percentage than commercial breeds.

Muscle fibers differ in their metabolic functions, with slow-twitch fibers being rich in mitochondria and aerobically efficient, while fast-twitch fibers are less so and rely more on glycolysis for energy production<sup>21</sup>. Consequently, metabolite profiles in muscles with varying fiber compositions are expected to be different. In the present study, the metabolite composition in the muscles of growing TB and XB pigs significantly differed from that of Duroc pigs. The differential metabolites were notably enriched in several pathways, including aspartate metabolism, malate-aspartate shuttle, and citric acid cycle. The activation of malate-aspartate shuttle is known to supply substrates for the citric acid cycle<sup>22</sup>. Moreover, the levels of malate-aspartate shuttle-related metabolites and gene expression have been shown to increase with the upregulation of PGC-1 $\alpha$  expression<sup>23</sup>, a condition that promotes the transformation from fast-twitch to slow-twitch muscle fibers<sup>24</sup>. Therefore, the metabolites related to the malate-aspartate shuttle might play a pivotal role in the muscle fiber type composition differences observed among the three pig breeds.

The higher roughage feeding tolerance is another distinguishing trait of many native pig breeds, setting them apart from commercial breeds. Our earlier research findings demonstrated that when fed a high-fiber diet, TB pigs achieved a higher average daily weight gain than Duroc pigs<sup>25</sup>. Pigs, being monogastric animals, depend on the distinct gut microbiota composition to break down dietary fibers<sup>26</sup>. It has been observed that the gut microbiota of native pigs significantly diverges from that of commercial pigs. The present study revealed that the colonic microbiota composition of growing TB and XB pigs significantly differed from Duroc pigs, with a notably higher abundance of *Lactobacillus* in the colon of TB and XB pigs. Consistent with our findings, the gut microbiota of Congjiang miniature pigs markedly differed from that of DLY pigs, with predominant abundances of the *Bacteroidaceae*, *Porphyromonadaceae*, and *Desulfovibrionaceae* families<sup>27</sup>. Similarly, the gut microbiota of growing Tibetan pigs differed significantly from that of DLY pigs at the genus level, with a notable enrichment of *Lactobacillus* and *Solibacillus*<sup>28</sup>. These findings suggest that the gut microbiota profiles of native pig breeds are generally distinct from commercial breeds.

Research on the gut-muscle axis has highlighted the substantial influence of gut microbiota on skeletal muscle<sup>29</sup>, yet the relationship between the distinct muscle fiber composition in native vs. commercial pig breeds and their gut microbiota remains unclear. Our study revealed a positive correlation between the abundance of *Lactobacillus* and the slow-twitch fiber percentage, suggesting a potential regulatory role of *Lactobacillus* in

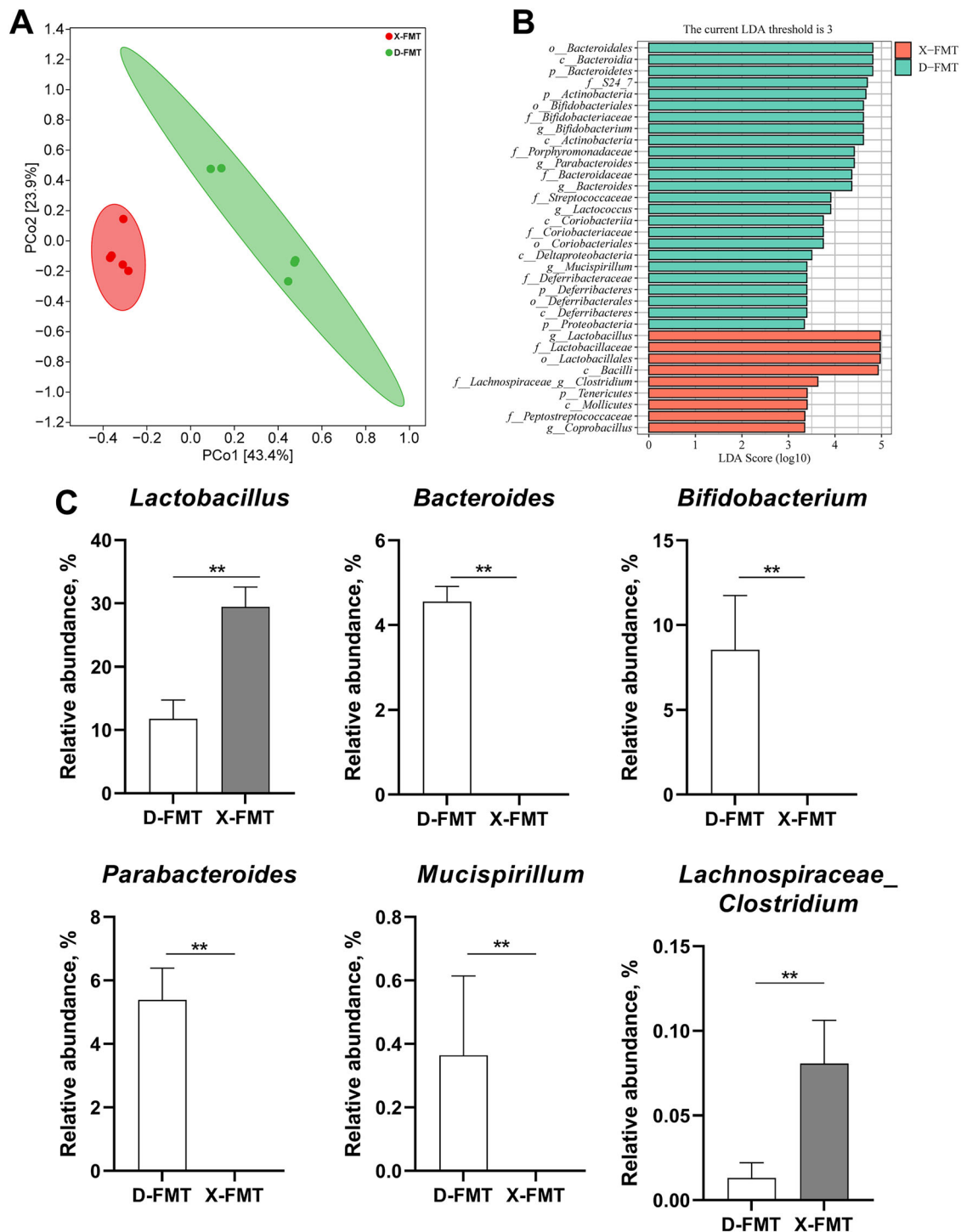


**Fig. 7 | The effects of FMT from XB and Duroc pigs on colonic microbiota of mice ( $n = 5$ ).** Data are presented as means with SD. **A** Principal coordinates analysis (PCoA) score plots of colonic microbiota, **B** linear discriminant analysis effect size (LEfSe) of colonic microbiota, and **C** taxonomic differences of colonic microbiota.

\*\* $P < 0.01$  (Mann-Whitney test). D-FMT mice received fecal microbiota transplantation from Duroc pigs at 125 days of age, and X-FMT mice received fecal microbiota transplantation from Xiangcun black (XB) pigs at 125 days of age.

slow-twitch fiber formation. To explore this hypothesis, we analyzed the colonic metabolite composition among three pig breeds at different ages. The results showed significant enrichment of differential metabolites in the tryptophan metabolism. Notably, the kynurenine pathway, a branch of tryptophan metabolism<sup>30</sup>, has been recognized for supporting the malate-aspartate shuttle in skeletal muscle, which is essential for adaptations to endurance exercise and enhancing fatigue resistance<sup>23</sup>. Moreover, kynurenine

acid has been previously reported to boost *PGC-1 $\alpha$*  expression and cellular respiration via *GPR35* activation in adipose tissue<sup>31</sup> and mitigate inflammation and insulin resistance in skeletal muscle tissues through *GPR35/AMPK* and *Sirt6*-mediated pathways<sup>32</sup>. The activation of the *AMPK/PGC-1 $\alpha$*  pathway is a key regulator of mitochondrial biogenesis and muscle fiber type transition<sup>33</sup>, implying that kynurenine acid might facilitate the development of slow-twitch fibers. This prompted us to investigate the *AMPK*

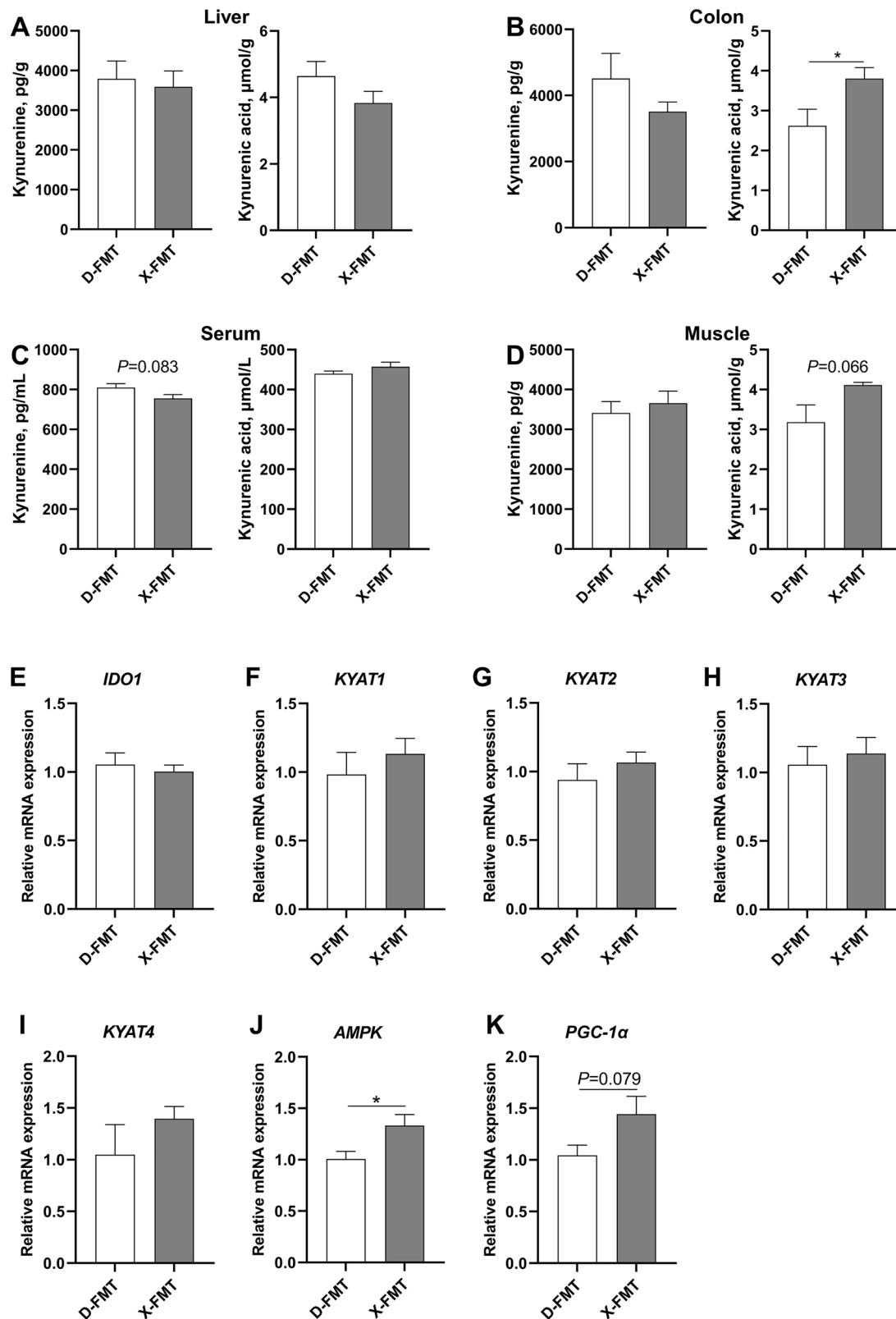


**Fig. 8 | The effects of FMT from XB and Duroc pigs on kynurenine and kynurenic acid concentrations and gene expressions in mice ( $n = 5$ ).** Data are presented as means with SD. Kynurenine and kynurenic acid concentrations in **A** liver, **B** colon, **C** serum, and **D** muscle. The mRNA expressions of **E** indoleamine 2,3-dioxygenase 1 (*IDO1*), **F** kynurenine aminotransferase1 (*KYAT1*), **G** *KYAT2*, **H** *KYAT3*, **I** *KYAT4*,

**J** protein kinase AMP-activated catalytic subunit alpha 1 (*AMPK*), and **K** peroxisome proliferator-activated receptor gamma coactivator 1 alpha (*PGC-1 $\alpha$* ) in muscle. \* $P < 0.05$  (Students' *t* test). D-FMT mice received fecal microbiota transplantation from Duroc pigs at 125 days of age, and X-FMT mice received fecal microbiota transplantation from Xiangcun black (XB) pigs at 125 days of age.

and *PGC-1 $\alpha$*  expressions in muscle tissue to elucidate the underlying molecular mechanisms linking gut microbiota to muscle fiber composition. Our results indicated that the muscle tissues of TB and XB pigs exhibit increased *PGC-1 $\alpha$*  expression compared to Duroc pigs, with *AMPK* expression also showing a similar upregulated trend. These observations suggest that the elevated level of kynurenic acid in TB and XB pigs could be a contributing factor to higher percentage of slow-twitch fibers in their muscles relative to Duroc pigs.

The correlation analysis revealed that *Lactobacillus* is a core genus associated with tryptophan metabolism and positively correlated with kynurenic acid. Interestingly, *Lactobacillus*, recognized for its probiotic properties, has been reported to preferentially synthesize kynurenic acid from kynurenine, which is then released extracellularly<sup>34</sup>. Studies have shown that the oral administration of certain *Lactobacillus* strains, such as *Lactobacillus plantarum* WSJ-06<sup>35</sup> or *Lactobacillus helveticus* WHH1889<sup>36</sup>, decreased serum kynurenine level while increasing kynurenic acid level in mice. In the present study, the abundance of *Lactobacillus* in the colon of TB and XB pigs was significantly higher than in Duroc pigs. Consequently, the kynurenic acid concentration in the colon, serum, and muscle of TB and XB pigs was higher than that of Duroc pigs. These findings suggest that the elevated kynurenic acid level in tissues of TB and XB pigs might have been attributed to the higher abundance of *Lactobacillus* present in the colon of TB and XB pigs.

Kynurenic acid, derived from the catabolism of tryptophan via the kynurenine pathway, is primarily synthesized in peripheral tissues by enzymes such as IDO1 and the four isozymes of KYATs (KYAT1–4)<sup>37</sup>. Gene expression analysis in muscles of three pig breeds did not reveal significant differences in the expression levels of these enzymes. This finding dismisses the idea that the elevated kynurenic acid level in TB and XB pigs is due to enhanced activity of the kynurenine pathway in the muscle tissue. Instead, these results support the hypothesis that the higher kynurenic acid level is a result of metabolic production by *Lactobacillus* in the gut. Given this evidence, along with the known role of kynurenic acid in promoting the *AMPK/PGC-1 $\alpha$*  pathway, we propose that by enhancing the production of kynurenic acid, *Lactobacillus* may indirectly stimulate the *AMPK/PGC-1 $\alpha$*  signaling pathway, thus facilitating the formation of slow-twitch fibers.

The FMT experiment was then conducted to verify the hypothesis mentioned earlier. The selection of XB pigs at 125 days of age was due to the colonic *Lactobacillus* abundance exceeding 80%, significantly higher than that of the Duroc pigs. The main goal was to assess the impact of these microbes on muscle fiber composition in mice. The results showed that the *MyHC IIa* expression in the *gastrocnemius* muscle of X-FMT mice was significantly higher compared with D-FMT mice. Additionally, there was a noticeable increasing trend in slow-twitch fiber percentages and upregulated *MyHC I* expression in X-FMT mice. The X-FMT mice also exhibited an increased abundance of *Lactobacillus* in the colon, similar to the colonic microbiota profile of the XB pigs. The kynurenic acid level in the colonic contents and muscle, as well as the activation of *AMPK/PGC-1 $\alpha$*  pathway in the *gastrocnemius* muscle, were significantly higher or tended to be higher in X-FMT mice. These findings align with a previous study, where mice receiving fecal microbiota from Chinese native Rongchang pigs also inherited the trait of higher slow-twitch fiber percentage<sup>38</sup>. Furthermore, X-FMT mice displayed a decreasing trend in serum kynurenine level, consistent with a previous study that reported a decline in serum kynurenine following oral *Lactobacillus plantarum* 299 v treatment in human<sup>39</sup>. Thus, our study provides compelling evidence that the higher abundance of colonic *Lactobacillus* in the XB pigs contributes to the higher slow-twitch fiber percentage in the muscle.

In conclusion, our study reveals a gut-muscle axis mediated by *Lactobacillus* and kynurenic acid, which modulates *AMPK/PGC-1 $\alpha$*  signaling to influence skeletal muscle fiber type composition. These findings establish a link between gut microbiota, tryptophan metabolism, and muscle physiology in Chinese native pigs. This mechanistic insights may inform future research on microbial interventions aimed at improving muscle quality in commercial pigs.

## Methods

### Ethics Statement

The animal experiments were approved by the Animal Care Committee of the Institute of Subtropical Agriculture, Chinese Academy of Sciences (Approval no. 20200018).

### Animals and Sample Collection

Forty-eight pigs (16 TB, 16 XB, and 16 Duroc pigs) at 30 days of age were selected for this study. All pigs were raised in the same pig house and fed the same diet until 125 days of age to minimize the effects of dietary and environmental factors. At 80 and 125 days of age, eight pigs per breed were fasted for 12 h, then euthanized by intramuscular injection of Zoletil® 50 (Beijing Lab Anim Tech Develop Co., Ltd., Beijing, China). The sample size and anesthesia method were determined based on our previous study<sup>40</sup>. After exsanguination, the samples of serum, *longissimus dorsi* (LD) muscle, liver, and colonic content were collected and stored at  $-80^{\circ}\text{C}$  for further analysis.

Twelve 6-week-old male C57BL/6 J mice were randomly divided into two groups based on body weight and received FMT from XB or Duroc pigs at 125 days of age, respectively. The mice were raised under standard conditions (12-h light/dark cycle, temperature  $22 \pm 2^{\circ}\text{C}$ , and humidity 50–60%) with *ad libitum* access to food and water. After antibiotic administration for two weeks, the mice received FMT from XB (X-FMT) and Duroc (D-FMT) pigs every day for a week. During the FMT process, one mouse died in each group, resulting in a final number of five mice per group as replicates. Then, all mice were raised normally for five weeks. All mice were anesthetized via intraperitoneal injection of 50 mg/kg sodium pentobarbital (Sigma-Aldrich, P3761, Shanghai, China), and then euthanized by cervical dislocation. Then serum, *gastrocnemius* muscle, liver, and colonic contents samples were collected.

### Muscle fiber type analysis

The LD muscle samples from pigs and *gastrocnemius* muscle samples from mice, stored with 4% paraformaldehyde, were embedded in a paraffin embedding medium (Servicebio, Wuhan, China) and then cut into 10  $\mu\text{m}$  slices using a pathology microtome (Leica, Wetzlar, Germany). Afterward, the paraffin sections were dewaxed with xylene and ethanol. The dewaxed sections were incubated in an EDTA antigen retrieval solution (Servicebio, G1206) to retrieve the antigen. After blocking with BSA (Servicebio, G5001), the sections were incubated with the first primary antibody mouse anti-slow myosin heavy chain (MyHC; AFbio, AF301061, Changsha, China) at  $4^{\circ}\text{C}$  overnight, followed by incubation with goat anti-mouse IgG (H + L)-Cy3 (AFbio, SA006) under dark condition. After that, the sections were incubated with the second primary antibody, mouse anti-fast MyHC (AFbio, SAF003), followed by incubation with goat anti-mouse IgG (H + L)-Alexa Fluor® 488 (AFbio, SA005). After drying, the sections were mounted with an anti-fluorescence quenching mounting medium (Servicebio, G1401). Finally, the sections were observed under a fluorescence microscope (Nikon, Tokyo, Japan), and images were collected. The muscle fiber characteristics, including fiber type, number, and cross-sectional area, were measured using Image-Pro Plus 6.0 (Media Cybernetics, Rockville, MD, USA).

### Targeted Metabolomics Analysis of LD muscles

The analysis of metabolite profiles of the LD muscles were performed by the Beijing Genomics Institute (BGI), Shenzhen, China, as previously described methods by Xie et al.<sup>15</sup>. Briefly, 10 mg of muscle sample was mixed with a 50% methanol/water solution, crushed, and centrifuged to collect the supernatant. A 96-well plate was filled with the supernatant, a working standard solution, an internal standard solution, and a freshly prepared derivative reagent. The plate was sealed and incubated at  $30^{\circ}\text{C}$  for 60 min to allow derivatization. After diluting the samples and cooling them at  $-20^{\circ}\text{C}$  for 20 min, the sample solutions were centrifuged at  $4000 \times g$  and  $4^{\circ}\text{C}$  for 30 min. The supernatant was then transferred to a new 96-well plate for LC-MS analysis using an ACQUITY BEH C18 column (1.7  $\mu\text{m}$ , 100 mm  $\times$  2.1 mm; Waters, Milford, MA, USA). The mass spectrometer operated in both positive and negative ion modes, with specific conditions set for



capillary voltage, source temperature, dissolution temperature, and gas flow as previously described<sup>15</sup>. Skyline software was used to automatically identify and integrate ion pairs, with a manual check for accuracy. The metabolite concentration ( $\mu\text{mol/g}$ ) was calculated as  $C \times A/m$ , where  $C$  is the concentration from the calibration curve,  $A$  is the dilution factor (0.14), and  $m$  is the mass of the sample. The partial least squares-discriminant analysis (PLS-DA) was conducted to assess the composition of muscular metabolites. Differential metabolites were identified as those with a  $P$ -value  $< 0.05$  based on Tukey's *post-hoc* test. Duroc pigs were designated as the control group, and pathway enrichment analysis was performed on muscle metabolites. Pathways with a false discovery rate (FDR)  $< 0.05$  were classified as significantly enriched pathways. Both the PLS-DA and pathway enrichment analysis for targeted metabolome were performed using the MetaboAnalyst tools at <https://www.metaboanalyst.ca/>, according to the online protocols<sup>41</sup>.

### Colonic microbiota analysis

16S rRNA gene sequencing of the colonic microbiota was performed by the Personal Biotechnology Co., Ltd., Shanghai, China. The total DNA of colonic content was extracted using commercial kits from TransGen Biotech. (Beijing, China), following the provided protocol. The V3–V4 regions of the 16S rRNA genes were amplified with universal forward primer 338F (5'-ACTCCTACGGGAGGCAGCA-3') and reverse primer 806R (5'-G GACTACHVGGGTWTCTAAT-3'). Quantification of PCR products was obtained using a microplate reader after fluorescent labeling. Bioinformatics analysis was conducted using QIIME2, which involved demultiplexing, primer trimming with cutadapt, and quality control using DADA2 for denoising and chimera removal. The taxonomy of amplicon sequence variants (ASVs) was assigned with the SILVA 132 database using the classify-sklearn classifier. The alpha-diversity indices, including Chao1, Observed species, Shannon, Simpson, Faith's PD, Pielou's evenness, and Good's coverage, were calculated using the QIIME2 software for each sample. The beta-diversity was analyzed using Bray-Curtis distances and visualized with principal coordinates analysis (PCoA). The linear discriminant analysis (LDA) effect size (LEfSe) method was used to identify differentially abundant taxa with an LDA score threshold of  $> 3$ . The advanced correlation link plots were performed using the OmicStudio tools at <https://www.omicstudio.cn/tool>.

### Colonic metabolite analysis

Colonic contents samples were processed according to previously described protocols<sup>16</sup>. Untargeted metabolomics analysis was performed by BioNovoGene Co., Ltd. (Suzhou, China). The raw data were converted into mzXML format using Proteowizard software (version 3.0.8789). Peak identification, filtration, and alignment were then conducted using the XCMS package for R (version 3.3.2). Metabolite annotation was achieved through cross-referencing LC-MS data with the Metlin database, the Human Metabolome Database (HMDB), and the mzcloud database. A final validation step was performed against BioNovoGene's in-house metabolite database to identify key metabolites. To investigate differences in metabolite profiles among the groups, PLS-DA was conducted in the MetaboAnalyst platform. Metabolites were considered differential if the  $P$ -value from one-way ANOVA was  $< 0.05$ . Furthermore, the pathway analysis was performed on these differential metabolites using MetaboAnalyst tools to uncover their biological relevance.

### Concentrations of kynurenine and kynurenic acid analysis

The concentrations of kynurenine (RC-12836M1) and kynurenic acid (RC-12837M1) in serum, colonic contents, liver, and muscle tissues were determined using commercial assay kits purchased from Huyu Biological Technology Co., Ltd. (Shanghai, China), following the manufacturer's protocol.

### Gene expression analysis

The total RNA in muscle tissue was extracted using TRIzol reagent (AG21101; Accurate Biology, Changsha, China) following the manufacturer's protocols. The concentration and purity of extracted RNA

were assessed with a NanoDrop ND-1000 spectrophotometer (Thermo Scientific, Waltham, MA, USA). Subsequently, 1000 ng of extracted RNA was reverse transcribed to cDNA using the Evo M-MLV RT Kit (Accurate Biology, AG11705, Changsha, China). The targeted gene expression was quantified by SYBR® Green Premix Pro Taq HS qPCR Kit (Accurate Biology, AG11701) on a LightCycler 480II Real-Time PCR System (Roche, Basel, Switzerland), following the kit and system instructions. The gene expression levels were normalized to the reference gene glyceraldehyde-3-phosphate dehydrogenase (GAPDH) using the  $2^{-\Delta\Delta Ct}$  method<sup>42</sup>. The target genes included protein kinase AMP-activated catalytic subunit alpha 1 (AMPK), indoleamine 2,3-dioxygenase 1 (IDO1), kynurenine aminotransferase (KYAT) 1–4, *MyHC I*, *MyHC IIa*, *MyHC IIx*, *MyHC IIb*, and peroxisome proliferator-activated receptor gamma coactivator 1 alpha (*PGC-1 $\alpha$* ). Primer sequences are listed in Table 2.

### Fecal microbiota transplantation

The bacterial solution for FMT was prepared using a previously established method<sup>43</sup>. The preparation of FMT is summarized as follows: 30 g of colonic contents from XB and Duroc pigs at 125 days of age were collected and diluted with 150 mL of sterile saline, and then homogenized using a blender. The resulting slurry was filtered through gauze and 0.25 mm stainless steel sieves three times to remove undigested material and small particulates. The suspension was centrifuged at  $6,000 \times g$  for 15 min. The precipitate was resuspended in sterile saline. Glycerol was added to the suspension to achieve a final concentration of 10%. The bacterial solution was transferred into 1.5 mL tubes and immediately stored at  $-80^\circ\text{C}$  to ensure microbial viability. The frozen bacterial solution was thawed at  $37^\circ\text{C}$  in a water bath, prior to FMT.

### Serum biochemical parameters analysis

Serum biochemical parameters were assessed using commercial kits from Leadman Biochemistry Technology Company (Beijing, China) and analyzed on a Cobas c311 Automatic Biochemical Analyzer (Roche, Basel, Switzerland), following the manufacturer's instructions. The serum biochemical parameters included albumin (ALB), alanine aminotransferase (ALT), aspartate aminotransferase (AST), cholinesterase (CHE), cholesterol (CHO), creatine kinase (CK), creatinine (CREA), high-density lipoprotein-cholesterol (HDL-C), lactic acid (LA), lactate dehydrogenase (LDH), low-density lipoprotein-cholesterol (LDL-C), lipase (LIP), ammonia (AMM), triglycerides (TG), total protein (TP), and urea nitrogen (UN).

### Forelimb grip strength test

A grip strength meter (DB025X, Zhishuduobao Biological Technology Co., Ltd., Beijing, China) was used to evaluate the forelimb grip strength of mice. The procedure involved lifting each mouse by the tail, encouraging it to grip a rigid grid connected to a digital force gauge. The tail was gently pulled to induce grip release, with the gauge recording the peak tension as the grip strength. Each mouse underwent five consecutive trials, and the mean grip strength (N) was determined from these measurements.

### Limitations

This study has two major methodological limitations. Firstly, the 16S rRNA sequencing approach used for gut microbiota profiling does not provide species-level resolution, and the FMT validation method cannot definitively confirm the functional roles of specific bacterial species. Secondly, the use of pseudo-germ-free mice employed in this study may result in less pronounced experimental outcomes compared to studies utilizing germ-free mice. These limitations underscore the need for methodological refinement in future research to address these challenges.

### Statistical analysis

Data are presented as means with standard deviation (SD) or standard error of the mean (SEM). The experimental unit is the single animal. The gut

Table 2 | Primers for real-time quantitative PCR used in the present study

Gene names	Primers	Sequences (5'–3')	Product size (bp)
Gene primers for pig			
AMPK	Forward	TTCGGCAAAGTGAAGTTTGG	224
	Reverse	AGCTCGCCTCCTGAAACATA	
GAPDH	Forward	GGAGCGAGATCCCGCCAACA	158
	Reverse	ACATGGGGGCATCGGCAGAA	
IDO1	Forward	CTCCGTCCTGTAGTTTGTTC	174
	Reverse	GAAGGCTCTTCGGATGCTTG	
KYAT1	Forward	AGGGCAGCTACTTCCTCATC	250
	Reverse	CACCTTCTGCAGCTTCTCGTC	
KYAT2	Forward	AGATGCAAGAAACCCCGAGA	181
	Reverse	GGGCTTGTTGAAGTCAGAA	
KYAT3	Forward	GGACAGCAGCGAACCTTATG	166
	Reverse	AGCAGCATCCAGTGTAGTGT	
KYAT4	Forward	GTAATTCTCTGCACGCCTG	155
	Reverse	TCCTTGTTACCATCGCCACT	
MyHC I	Forward	GGCCCCCTCCAGCTTGA	63
	Reverse	TGGCTGCGCCTTGGTTT	
MyHC IIa	Forward	TTAAAAAGCTCCAAGAACTGTTCA	100
	Reverse	CCATTTCTGGTGCGAACTC	
MyHC IIb	Forward	CACTTTAAGTAGTTGTCTGCCTTGAG	80
	Reverse	GGCAGCAGGGCACTAGATGT	
MyHC IIx	Forward	AGCTTCAAGTTCTGCCCACT	76
	Reverse	GGCTGCGGGTTATTGATGG	
PGC-1α	Forward	GCCCAGTCTCGCGCTATTT	265
	Reverse	GTTCACTCGGCTCGGATTT	
Gene primers for mice			
AMPK	Forward	CTCAACCGGCAGAAGATTCTG	212
	Reverse	CGGCTTTCCTTTTCGTCCAA	
GAPDH	Forward	GGGTCCCAGCTTAGGTTTCAT	248
	Reverse	CATTCTCGGCCTTGACTGTG	
IDO1	Forward	TCTCAGAGAAGTTGGGCCTG	189
	Reverse	CAGGAGAAGCTGCGATTTC	
KYAT1	Forward	GGCAGCTACTTCTCAATTGC	169
	Reverse	CCTTATGATGGGGCTGGCTA	
KYAT2	Forward	CCCATCAGAAGTACAGCGGA	163
	Reverse	GGGCCCTTTTGATCAAGTCG	
KYAT3	Forward	TCATTGCTGACCTTTGCGTC	152
	Reverse	TGCTTGCCAGCACTTCTTA	
KYAT4	Forward	CAGCCGAGATGTCTTTCTGC	167
	Reverse	GGACACTCTGCTCTGGGATT	
MyHC I	Forward	AGACGGTGACTGTGAAGGAG	202
	Reverse	TACACAGGCAGCCACTTGTA	
MyHC IIa	Forward	CAGTGCTAAGGCCAAGGGA	171
	Reverse	TCTCATCAAGCTGCCTGGAA	
MyHC IIb	Forward	TTGAAAGACGAAGCAGCGAC	190
	Reverse	AGAGAGCGGGACTCCTCTG	
MyHC IIx	Forward	GCGAATCGAGGCTCAGAACAA	138
	Reverse	GTAGTTCCGCCTTCGGTCTTG	
PGC-1α	Forward	AGCCTCTTTGCCAGATCTT	241
	Reverse	GGCAATCCGCTTTCATCCAC	

Abbreviations: AMPK, protein kinase AMP-activated catalytic subunit alpha 1; GAPDH, glyceraldehyde-3-phosphate dehydrogenase; IDO1, indoleamine 2,3-dioxygenase 1; KYAT, kynurenine aminotransferase; MyHC, myosin heavy chain; PGC-1α, peroxisome proliferator-activated receptor gamma coactivator 1 alpha.

microbiota data from TB, XB, and Duroc pigs were assessed using the Kruskal-Wallis test. The comparisons between X-FMT and D-FMT mice were performed using the Mann-Whitney test. For other datasets, statistical differences among TB, XB, and Duroc pigs were evaluated using one-way ANOVA, followed by Tukey’s post hoc test for multiple comparisons. The comparisons between X-FMT and D-FMT mice were performed using the Student’s *t* test. A *P* value < 0.05 was considered to indicate statistical significance. 0.05 ≤ *P* < 0.1 indicated a trend toward significant differences. All statistical analyses were conducted using SPSS software (version 22.0; SPSS Inc., Chicago, IL, USA). Throughout allocation, experimental conduct, outcome assessment, and data analysis, only Bo Song and Xiangfeng Kong were aware of the group allocation.

Data availability

Sequence data that support the findings of this study have been deposited in the ScienceDB (<https://www.scidb.cn/en/s/mEjquu>).

Received: 5 November 2024; Accepted: 2 June 2025;  
Published online: 23 June 2025

References

- Gagaoua, M. & Picard, B. Muscle fiber properties in cattle and their relationships with meat qualities: An overview. *J. Agric. Food Chem.* **68**, 6021–6039 (2020).
- Joo, S. T., Kim, G. D., Hwang, Y. H. & Ryu, Y. C. Control of fresh meat quality through manipulation of muscle fiber characteristics. *Meat Sci.* **95**, 828–836 (2013).
- Choe, J. H. & Kim, B. C. Association of blood glucose, blood lactate, serum cortisol levels, muscle metabolites, muscle fiber type composition, and pork quality traits. *Meat Sci.* **97**, 137–142 (2014).
- Guo, J. et al. Comparisons of different muscle metabolic enzymes and muscle fiber types in Jinhua and Landrace pigs. *J. Anim. Sci.* **89**, 185–191 (2011).
- Huang, Y. N. et al. Comparisons of different myosin heavy chain types, AMPK, and PGC-1α gene expression in the *longissimus dorsi* muscles in Bama Xiang and Landrace pigs. *Genet. Mol. Res.* **15**, gmr.15028379 (2016).
- Park, B. Y., Kim, N. K., Lee, C. S. & Hwang, I. H. Effect of fiber type on postmortem proteolysis in longissimus muscle of Landrace and Korean native black pigs. *Meat Sci.* **77**, 482–491 (2007).
- Yang, H. et al. Gut microbiota is a major contributor to adiposity in pigs. *Front. Microbiol.* **9**, 3045 (2018).
- Mancin, L., Wu, G. D. & Paoli, A. Gut microbiota-bile acid-skeletal muscle axis. *Trends Microbiol.* **31**, 254–269 (2023).
- Lahiri, S. et al. The gut microbiota influences skeletal muscle mass and function in mice. *Sci. Transl. Med.* **11**, eaan5662 (2019).
- Chen, L. H. et al. Probiotic supplementation attenuates age-related sarcopenia via the gut-muscle axis in SAMP8 mice. *J. Cachexia Sarcopenia Muscle* **13**, 515–531 (2022).
- Qi, R. et al. The intestinal microbiota contributes to the growth and physiological state of muscle tissue in piglets. *Sci. Rep.* **11**, 11237 (2021).
- Xu, G. et al. The influence of increasing roughage content in the diet on the growth performance and intestinal flora of Jinwu and Duroc × Landrace × Yorkshire pigs. *Animals* **14**, 1913 (2024).
- Ma, J. et al. Gut microbial profiles and the role in lipid metabolism in Shaziling pigs. *Anim. Nutr.* **9**, 345–356 (2022).
- Yin, J. et al. Obese Ningxiang pig-derived microbiota rewires carnitine metabolism to promote muscle fatty acid deposition in lean DLY pigs. *Innovation* **4**, 100486 (2023).
- Song, B. et al. Muscle characteristics comparison and targeted metabolome analysis reveal differences in carcass traits and meat quality of three pig breeds. *Food Funct.* **14**, 7603–7614 (2023).
- Ding, S. et al. Development of small intestinal barrier function and underlying mechanism in Chinese indigenous and Duroc piglets during suckling and weaning periods. *Anim. Nutr.* **16**, 429–442 (2024).

17. Lee, S. H., Joo, S. T. & Ryu, Y. C. Skeletal muscle fiber type and myofibrillar proteins in relation to meat quality. *Meat Sci.* **86**, 166–170 (2010).
18. Zhang, C. et al. Differential expression of lipid metabolism-related genes and myosin heavy chain isoform genes in pig muscle tissue leading to different meat quality. *Animal* **9**, 1073–1080 (2015).
19. Wimmers, K. et al. Relationship between myosin heavy chain isoform expression and muscling in several diverse pig breeds. *J. Anim. Sci.* **86**, 795–803 (2008).
20. Kim, N. K. et al. Comparisons of *longissimus* muscle metabolic enzymes and muscle fiber types in Korean and Western pig breeds. *Meat Sci.* **78**, 455–460 (2008).
21. Zhang, Y. et al. Butyrate promotes slow-twitch myofiber formation and mitochondrial biogenesis in finishing pigs via inducing specific microRNAs and PGC-1 $\alpha$  expression. *J. Anim. Sci.* **97**, 3180–3192 (2019).
22. Hatazawa, Y. et al. Metabolomic analysis of the skeletal muscle of mice overexpressing PGC-1 $\alpha$ . *PLoS ONE* **10**, e0129084 (2015).
23. Agudelo, L. Z. et al. Skeletal muscle PGC-1 $\alpha$ 1 reroutes kynurenine metabolism to increase energy efficiency and fatigue-resistance. *Nat. Commun.* **10**, 2767 (2019).
24. Zhang, L. et al. Skeletal muscle-specific overexpression of PGC-1 $\alpha$  induces fiber-type conversion through enhanced mitochondrial respiration and fatty acid oxidation in mice and pigs. *Int. J. Biol. Sci.* **13**, 1152–1162 (2017).
25. Liu, J. et al. Effects of dietary fiber on growth performance, nutrient digestibility and intestinal health in different pig breeds. *Animals* **12**, 3298 (2022).
26. Hu, R. et al. The interaction between dietary fiber and gut microbiota, and its effect on pig intestinal health. *Front. Immunol.* **14**, 1095740 (2023).
27. Hu, J. et al. Gut microbiota-derived 3-phenylpropionic acid promotes intestinal epithelial barrier function via AhR signaling. *Microbiome* **11**, 102 (2023).
28. Yang, Y. et al. Comparative study on jejunal immunity and microbial composition of growing-period Tibetan pigs and Duroc  $\times$  (Landrace  $\times$  Yorkshire) pigs. *Front. Vet. Sci.* **9**, 890585 (2022).
29. Xie, X. & Huang, C. Role of the gut-muscle axis in mitochondrial function of ageing muscle under different exercise modes. *Ageing Res. Rev.* **98**, 102316 (2024).
30. Agus, A., Planchais, J. & Sokol, H. Gut microbiota regulation of tryptophan metabolism in health and disease. *Cell Host Microbe* **23**, 716–724 (2018).
31. Agudelo, L. Z. et al. Kynurenic acid and GPR35 regulate adipose tissue energy homeostasis and inflammation. *Cell Metab.* **27**, 378–392.e375 (2018).
32. Jung, T. W. et al. Administration of kynurenic acid reduces hyperlipidemia-induced inflammation and insulin resistance in skeletal muscle and adipocytes. *Mol. Cell. Endocrinol.* **518**, 110928 (2020).
33. Zhang, J. et al. Effect of resveratrol on skeletal slow-twitch muscle fiber expression via AMPK/PGC-1 $\alpha$  signaling pathway in bovine myotubes. *Meat Sci.* **204**, 109287 (2023).
34. Schwarcz, R., Foo, A., Sathyaikumar, K. V. & Notarangelo, F. M. The probiotic *Lactobacillus reuteri* preferentially synthesizes kynurenic acid from kynurenine. *Int. J. Mol. Sci.* **25**, 3679 (2024).
35. Li, Y. et al. *Lactobacillus plantarum* WSJ-06 alleviates neurobehavioral injury induced by lead in mice through the gut microbiota. *Food Chem. Toxicol.* **167**, 113308 (2022).
36. Gao, K. et al. Improvements of age-related cognitive decline in mice by *Lactobacillus helveticus* WHH1889, a novel strain with psychobiotic properties. *Nutrients* **17**, 3852 (2023).
37. Zhen, D., Liu, J., Zhang, X. D. & Song, Z. Kynurenic acid acts as a signaling molecule regulating energy expenditure and is closely associated with metabolic diseases. *Front. Endocrinol.* **13**, 847611 (2022).
38. Yan, H. et al. Gut microbiota can transfer fiber characteristics and lipid metabolic profiles of skeletal muscle from pigs to germ-free mice. *Sci. Rep.* **6**, 31786 (2016).
39. Rudzki, L. et al. Probiotic *Lactobacillus Plantarum* 299v decreases kynurenine concentration and improves cognitive functions in patients with major depression: a double-blind, randomized, placebo controlled study. *Psychoneuroendocrinology* **100**, 213–222 (2019).
40. Ding, S. et al. Dietary fiber alters immunity and intestinal barrier function of different breeds of growing pigs. *Front. Immunol.* **14**, 1104837 (2023).
41. Pang, Z. et al. Using MetaboAnalyst 5.0 for LC-HRMS spectra processing, multi-omics integration and covariate adjustment of global metabolomics data. *Nat. Protoc.* **11**, 1735–1761 (2022).
42. Schmittgen, T. D. & Livak, K. J. Analyzing real-time PCR data by the comparative C(T) method. *Nat. Protoc.* **3**, 1101–1108 (2008).
43. Hu, J. et al. Standardized preparation for fecal microbiota transplantation in pigs. *Front. Microbiol.* **9**, 1328 (2018).

## Acknowledgements

This work was supported by the National Key Research and Development Project under grant (2023YFD1301305), National Natural Science Foundation of China under grant (32350410424), Future Partner Special Network Fund of Chinese Academy of Sciences under grant (092GJHZ2022044FN), Hunan Province Natural Science Foundation under grant (2022JJ30643), and Taishan industry leading talent project special funds.

## Author contributions

B.S.: investigation, writing-original draft, and editing. M.A.K.A.: funding, methodology, writing-review, and editing. Y.C. and S.D.: investigation and methodology. Q.Z. and K.Y.: funding, writing-review and editing. X.K.: conceptualization, investigation, funding, writing-review and editing.

## Competing interests

The authors declare no competing interests.

## Additional information

**Supplementary information** The online version contains supplementary material available at <https://doi.org/10.1038/s41522-025-00745-3>.

**Correspondence** and requests for materials should be addressed to Xiangfeng Kong.

**Reprints and permissions information** is available at <http://www.nature.com/reprints>

**Publisher's note** Springer Nature remains neutral with regard to jurisdictional claims in published maps and institutional affiliations.

**Open Access** This article is licensed under a Creative Commons Attribution-NonCommercial-NoDerivatives 4.0 International License, which permits any non-commercial use, sharing, distribution and reproduction in any medium or format, as long as you give appropriate credit to the original author(s) and the source, provide a link to the Creative Commons licence, and indicate if you modified the licensed material. You do not have permission under this licence to share adapted material derived from this article or parts of it. The images or other third party material in this article are included in the article's Creative Commons licence, unless indicated otherwise in a credit line to the material. If material is not included in the article's Creative Commons licence and your intended use is not permitted by statutory regulation or exceeds the permitted use, you will need to obtain permission directly from the copyright holder. To view a copy of this licence, visit <http://creativecommons.org/licenses/by-nc-nd/4.0/>.

© The Author(s) 2025